Electronic structure of Co-induced magic clusters grown on Si(111)-(7×7): Scanning tunneling microscopy and spectroscopy and real-space multiple-scattering calculations

M. A. K. Zilani, H. Xu, T. Liu, Y. Y. Sun, Y. P. Feng, X.-S. Wang, and A. T. S. Wee*
Department of Physics, National University of Singapore, Kent Ridge, Singapore 119260, Republic of Singapore
(Received 7 February 2006; published 17 May 2006)

The electronic structure of cobalt-induced magic clusters grown on Si(111)-(7×7) is investigated by scanning tunneling microscopy, scanning tunneling spectroscopy, and real-space multiple-scattering calculations. Topographical images of a half unit cell of Si(111)-(7×7) with the cluster acquired at low bias voltages of ±0.4 V show greatly reduced cluster heights; however, the heights of the corner adatoms are unchanged, indicative of the highly localized nature of the charge distribution. Spectroscopic studies of the clusters indicate a band gap of ~0.8 eV, suggesting localized nonmetallic behavior. The opening of such a band gap is suggested to be a stabilizing factor for the observed magic clusters. A 65-atom Co-Si cluster is constructed to calculate the momentum- and element-projected density of states. The calculated result identifies that the intense state below the Fermi level at −1.75 V in the experimental spectroscopic curve is primarily due to localized 3*d* orbitals of Co atoms in the magic clusters.

DOI: 10.1103/PhysRevB.73.195415 PACS number(s): 73.22.−f, 68.35.Bs, 68.37.Ef, 71.15.−m

I. INTRODUCTION

The Si(111)-(7×7) surface has been used as a natural template to grow nanodots of different elements with identical size and shape comprising a fixed number of atoms, i.e., magic clusters.[1–6] Such low-dimensional structures with interesting quantum properties not only are of fundamental scientific interest, but have a wide variety of potential nanotechnology applications. Perfectly ordered superlattices of nanodots on a wide area have been observed for Sn and group-III elements (In, Al, Ga, and Tl).[1–6] Clusters with well-defined atomic arrangement (within the cluster) have been achieved with elements such as Pb, Au, Ag, and Cu.[7–10] On the other hand, the 3*d* ferromagnetic metals Ni, Co, and Fe are highly reactive with Si and involve rearrangement of substrate atoms, making it difficult to achieve formation of identical clusters while keeping intact the Si(111)-(7×7) periodicity.[11,12] Recently we reported the formation of Co-induced magic clusters: two characteristic adatom vacancies observed with every cluster and the off-center position within the 7×7 half unit cell (HUC) make it a unique system for studying nanostructural self-assembly.[13]

Due to the partially filled Si adatom intrinsic surface states, Si(111)-(7×7) is metallic at room temperature.[14] Nanodots formed by elements such as Tl [at ~0.2 monolayer (ML) coverage] preserve the metallic character of this surface.[4] However, for other elements such as Al, Sn, In, and Pd, the surface becomes nonmetallic due to removal of dangling bond states at the Fermi energy. At ~0.1 ML coverage of Sn and ~0.33 ML coverage of Ag, a gap of ~1.0 eV opens about the Fermi energy.[1,15] Only above certain coverages do these clusters show metallic behavior. In this paper, the electronic structure of cobalt-induced magic clusters grown on Si(111)-(7×7) at 0.06 ML coverage is investigated by scanning tunneling microscopy (STM), scanning tunneling spectroscopy (STS) and real-space multiple-scattering (RSMS) calculations.[16] Spectroscopic studies on the clusters indicate localized *nonmetallic* characteristics with a band gap of ~0.8 eV. STM images reveal the clusters with greatly reduced height at low bias voltages of ±0.4 V; however, the heights of three corner adatoms in that HUC are unchanged, indicative of the highly localized nature of the charge distribution and further support the nonmetallic behavior. The calculated momentum- and element-projected densities of states (DOSs) identify the intense state at −1.75 V below the Fermi level in experimental spectroscopic curve as primarily due to localized 3*d* orbitals of Co atoms in the magic clusters.

II. EXPERIMENT

In situ experiments were performed in a multichamber ultrahigh-vacuum (UHV) system with a base pressure of 2×10^{-10} mbar.[17] The analysis chamber contains variable-temperature STM, x-ray photoelectron spectroscopy (XPS), and low-energy electron diffraction (LEED). Atomically clean Si(111)-(7×7) surfaces were prepared by degassing the sample at 500 °C overnight, and repeated flashing to 1200 °C. A polycrystalline tungsten wire with 0.38 mm diameter was etched electrochemically in NaOH and subsequently cleaned in ethanol and distilled water to produce sharp STM tips. High-purity (99.99%) Co was evaporated by an *e*-beam evaporator maintaining the chamber pressure below 1×10^{-9} mbar. The surface cleanliness and reconstruction were monitored regularly by XPS and LEED. A Co-coverage of ~0.06 ML (1 ML=7.83×10^{14} Co atoms/cm^2) and deposition temperature of 230±20 °C were found to be the optimal conditions to grow Co-induced magic clusters on a Si(111)-(7×7).[13]

III. RESULTS AND DISCUSSION

A. Bias-dependent STM imaging

Figure 1 is a high-resolution empty-state STM image showing Co-induced magic clusters on Si(111)-(7×7). *F* represents the faulted half unit cell (FHUC). The clusters are off-center within each HUC, and are accompanied by two

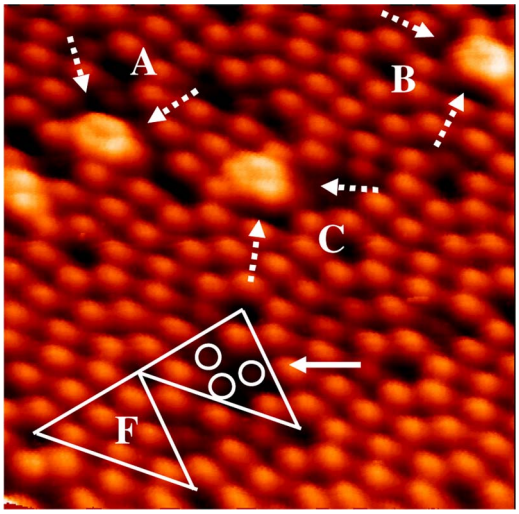

FIG. 1. (Color online) Empty-state STM image of a surface where in addition to magic clusters we also observe a 7×7 HUC with three missing center adatoms (shown by solid arrow). All these clusters and the three missing center adatoms are within the FHUC. The dotted arrows show the two center adatom vacancies associated with every cluster. There is some thermal drift in the image causing distortion.

center adatom vacancies (indicated by white dotted arrows) on either side within the HUC as previously reported.[13] There are three equivalent orientations of the magic cluster and adatom vacancies within a single FHUC marked as *A*, *B*, and *C* in Fig. 1. The solid arrow indicates a FHUC where all three center adatoms are missing, as marked by circles. We believe the clustering process was initiated at this FHUC but the cluster somehow was displaced or did not form. In an earlier study, we proposed a cluster model comprising three Si adatoms and six Co adatoms [shown in Fig. 4(a) below] to explain the observed STM images.[13]

Figures 2(a) and 2(b) show a series of empty- and filled-state STM images of the same Si(111)-(7×7) unit cell containing a magic cluster in the FHUC taken at bias voltages ±0.4, ±0.6, ±0.8, ±1.4, and ±2.0 V, respectively. Figure 2 reveals that even at low bias voltages of ±0.4 V, the adatoms in the unfaulted half unit cell (UFHUC) (i.e., with no cluster) are very clear due to appreciable tunneling current, indicating that the Si(111) adatoms are characterized by metallic surface states.[14,18] For filled-state STM topographs at negative biases higher than -0.8 V, not only are the contributions from the adatoms, but the rest atom dangling bond and back-bond states also become significant as clearly evident in the UFHUC of Fig. 2(b) at -1.4 and -2.0 V. In a recent study, Wang *et al.* used a sharp tungsten tip to observe both rest atoms and adatoms with equal brightness within the UFHUC at -1.5 V sample bias.[19] Sutter *et al.* observed similar features at -1.7 Vbias voltage using a InAs tip.[20] Moreover at -2.0 V bias their STM images map the rest atoms about 0.5 Å above the corner adatoms. The observation of adatoms as well as rest atoms (indicated by arrows) is clearly evident in Fig. 2(b) at -1.4 V. Moreover at bias voltage of -2.0 V, the rest atoms are about 0.3 Å above the corner adatoms in the UFHUC [Fig. 2(b)]. The reproducibility of these features[14,19,20] undoubtedly confirms that a sharp clean tip was used in our experiment and ensures the reliability of the magic cluster features at different bias voltages.

The height profiles between points *X* and *Y* as marked on the STM image acquired at +2.0 V are placed next to the corresponding STM images in Fig. 2. From the cross-sectional line profiles, the height of the clusters increases with increase of bias voltages in both empty- and filled-state STM images. The arrow at the line profile indicates the middle of the clusters. The cluster height is measured with respect to the corner adatom of the FHUC. At bias voltages ±0.4 V, the cluster is imaged as a depression 0.75 ± 0.05 Å (0.85 ± 0.05 Å) beneath the 7×7 adatoms in the empty-

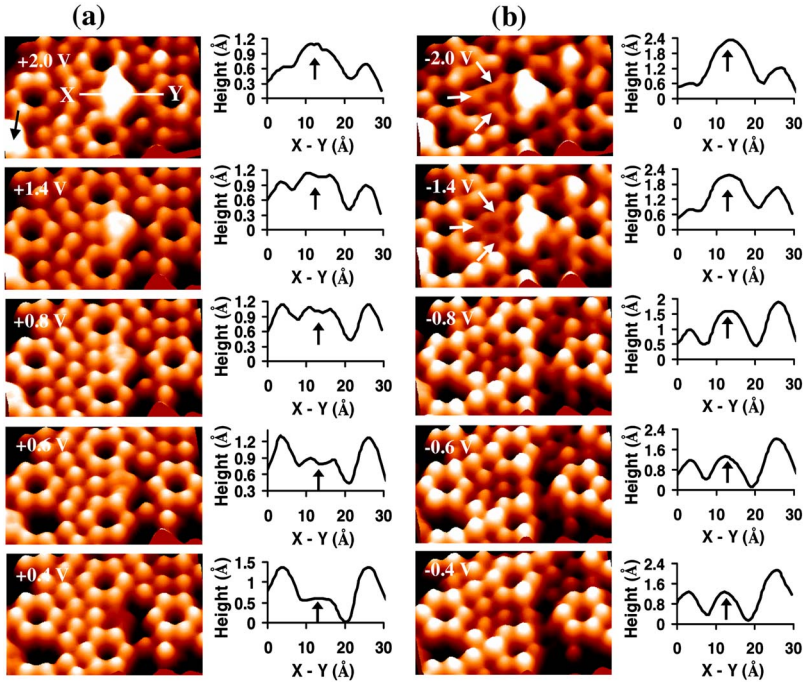

FIG. 2. (Color online) The left column shows empty- (a) and filled- (b) state STM images of a Si(111)-(7×7) unit cell comprising a Co-induced magic cluster in the FHUC at bias voltages ±0.4, ±0.6, ±0.8, ±1.4, and ±2.0 V, respectively. The arrow on the lower left corner at STM image of +2.0 V indicates an area which shows all the images are for the same area (i.e. cluster). The right column shows the cross-sectional line profile between two points *X* and *Y* as indicated in the image of +2.0 V. In the line profiles the middle of the clusters has been marked by an up arrow. Arrows on the filled-state STM images at -1.4 and -2.0 V indicate rest atoms in the UFHUC.

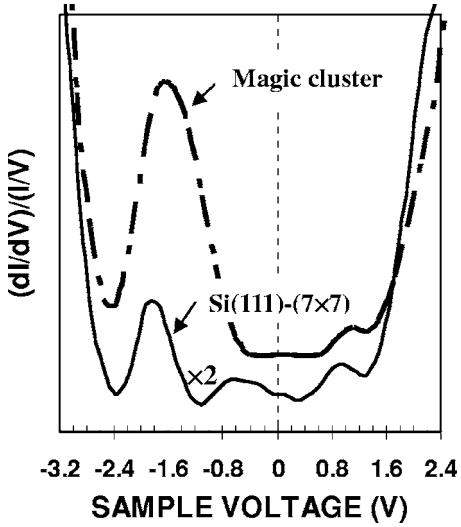

FIG. 3. STS measurements were performed at different places on the surface, and averaged $(dI/dV)/(I/V)$ versus V curves are shown by a solid (for Si surface area not covered with clusters) and dash-dotted (for magic clusters) lines, respectively.

(filled-)state STM image. The drastic reduction of cluster height (as opposed to the three corner adatoms within that HUC which are unchanged) is indicative of the localized nature of the charge distribution. At about ±1.0 V the cluster and corner adatoms appear approximately at the same height; however, at ±2.0 V the cluster height increases by 0.45±0.05 Å (0.95±0.05 Å) in the empty- (filled-)state images.

B. STS measurements

STS measurements shown in Fig. 3 were performed on the clusters and clean regions of the surface to determine the local density of states (LDOS). The normalized first derivative of the tunneling current, $(dI/dV)/(I/V)$, is roughly proportional to the LDOS.[21] This quantity is independent of the transmission factor and does not diverge for voltages close to zero.[21] Here, $(dI/dV)/(I/V)$ was numerically calculated by adding a small constant to the I/V values to overcome the problem due to divergence at the band edges.[22,23] The averaged $(dI/dV)/(I/V)$ versus V curves for the clean region and cluster are represented in Fig. 3 by a solid and dash-dotted lines, respectively. The Fermi level corresponds to 0 V and the energy of the surface states is measured by the sample voltage relative to the Fermi level. All STS curves were measured at the tip position corresponding to the tunneling condition of 2.0 V and 0.1 nA. Atomic resolution STM images (Fig. 2) acquired during STS measurements ensure an unchanged tip atomic (as well as electronic) structure and hence validates our STS results.

Earlier studies of clean Si(111)-(7×7) reported surface states at −0.4 and 0.5 V for partially filled adatom bands, −0.8 V for completely filled rest atoms, and −1.7 V for corner holes and Si-Si backbonds surrounding the adatoms.[14,18] The surface state observed at 1.3 V originates from exposed Si adatom backbonds in the surface double layer.[14,18] In this study we observe the surface states of the clean region (solid line in Fig. 3) at −0.35, −0.7, −1.8, and 0.95 V. These peaks can be assigned, respectively, to the partially filled adatom bands, completely filled rest atoms, corner hole and Si-Si backbonds surrounding the adatoms, and Si adatom backbonds in the surface double layer.

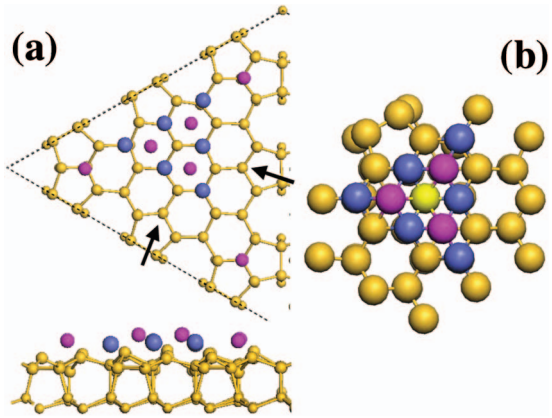

FIG. 4. (Color) (a) Top and side view of the Co-induced magic cluster in the FHUC (from Ref. 13). The Si and Co adatoms are indicated by pink and blue balls, respectively. The atoms in the rest atom layer and below are shown by yellow balls. Arrows indicate two center adatom vacancies associated with every cluster. (b) Top view of the cluster with 59 Si and six Co atoms constructed [based on relaxed cluster structure of Fig. 4(a)] for momentum- and element-projected DOS calculation. Here the light yellow ball is Si and considered as a central atom for the calculation.

The normalized conductivity on a magic cluster (dash-dotted line in Fig. 3) shows two states at −1.75 and 1.2 V, and a flat gap region from −0.3 to +0.5 V. The flat region may be associated with an energy gap around the Fermi energy. Qualitatively the gap extends from the valence-band maximum to conduction-band minimum and is indicative of nonmetalliclike behavior. Similar gaps were reported for In, Ag, and Sn clusters on Si(111)-(7×7),[1,2,15] and the Si_7In_6 magic cluster on Si(100).[24] There is a clear correspondence of this gap with STM images of the clusters acquired at low biases (±0.4 V), where the clusters are observed as depressions with respect to the Si adatoms. A small height corresponds to low density of states and further supports the nonmetalliclike behavior of the clusters. At ±0.4 V, a comparison between the two halves of Si(111)-(7×7) unit cell [STM images Figs. 2(a) and 2(b)] clearly indicates that the Co-induced clusters cause a reduction in density of states near the Fermi level.

At bias voltage ±2.0 V, the cluster height in the filled state is almost double that of the empty-state image. This results in the drastic increase of tunneling conductance below −0.3 V in the STS curve (where the occupied states are probed) with a peak at −1.75 V (dash-dotted line in Fig. 3). In the next section we will show that this peak is due predominantly to the LDOS from the second-layer Co atoms in the clusters. The cluster model is shown in Fig. 4(a).

C. RSMS calculations

To simulate the STS curves, we carried out DOS calculations using the FEFF8 code (version 8.20, University

of Washington),[16] which uses a RSMS approach with self-consistent muffin-tin (MT) potentials. A 37-atom cluster [6.1 Å radius around a central Si atom indicated in light yellow in Fig. 4(b)] was constructed for the self-consistent field potential calculation. The potentials and phase shifts were calculated with the absence of a core hole. The MT radii were overlapped by a factor of 1.15 to reduce the effects of discontinuities between adjacent regions of MT potentials. Nonoverlapping MT radii are determined automatically from the calculated Norman radii.[25] The full multiple-scattering calculations were performed for a Co-Si cluster shown in Fig. 4(b) which contains 59 Si and six Co atoms (8 Å radius from central Si atom). The cluster is constructed based on the relaxed structure of Fig. 4(a),[13] and the top view is shown in Fig. 4(b). The RSMS method can calculate atomic potentials self-consistently, providing an accurate Fermi energy (typically to within a fraction of 1 eV), as well as the orbital angular momentum projected DOS (*l*-DOS). The energy resolution and accuracy of DOS calculations are limited by broadening due to cluster size, self-energy, and lifetime contributions, and by the lack of full potential corrections to the MT potentials.[16]

The *l*-DOSs calculated from the 65-atom cluster are shown separately for Si and Co in Figs. 5(a) and 5(b), respectively. The 0 eV indicates the Fermi level E_F (shown by vertical dashed line). In Fig. 5(a) the dominant peaks below E_F can be attributed to the $3p$ character of Si. Despite broadened spectra around E_F, a gap can be roughly resolved indicating a nonmetalliclike behavior. The resolution of the Si *l*-DOS can be improved by including more atoms in the calculated cluster, but the main features remain basically the same. In Fig. 5(b), the dominant peak below E_F at -2.05 eV can be attributed to the localized Co $3d$ orbitals. The inset in Fig. 5(b) shows full $3d$ peak of the *l*-projected DOSs in the energy range -5 to 15 eV; the maximum value of Co $3d$ *l*-DOS is ~nine times higher than that of Si $3p$. The position of the large peak in the STS curve at -1.75 V (dash–dotted line in Fig. 3) is comparable to the dominant Co $3d$ peak in Fig. 5(b). Moreover, the band gap evident from the Si-$3p$-projected DOS is consistent with the observed gap in the STS curve in Fig. 3.

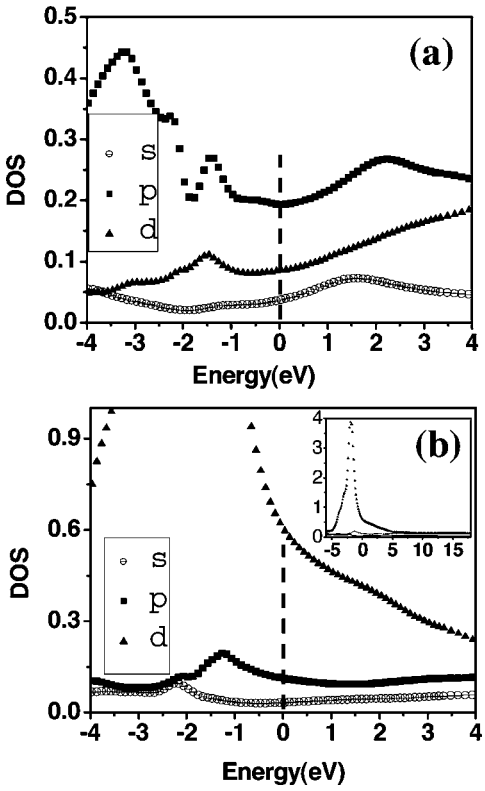

FIG. 5. The *s*-, *p*-, and *d*-projected *l*-DOSs (shown by circle, square, and triangle marks, respectively) for Si (a) and Co (b). Here 0 eV indicates the Fermi level and is marked by a vertical dashed line. The inset in (b) indicates the DOS using a larger scale.

IV. CONCLUSIONS

The electronic structure study of low-dimensional systems such as $3d$ ferromagnetic metal-induced clusters is important for understanding their electrical, optical, and magnetic properties.[26] The STS results suggest that the magic clusters are responsible for a local removal of the metallicity of Si(111)-(7×7) and a band gap of 0.8 eV opens near the Fermi energy. This band gap opening suggests the gain of electronic energy as a driving force for the formation of the magic clusters. The significant increase in cluster height starting at a bias of -0.8 V in filled-state STM images is consistent with a drastic increase of tunneling conductance below the Fermi level in the STS curve, with a maximum at -1.75 V. From the momentum- and element-projected DOS calculations, it is clear that this peak is due to Co atoms at the second layer of the magic cluster. Such a systematic understanding of the interface and electronic structure is important for future applications of nanodevices using metal clusters.

*Corresponding author. FAX: +65-67776126. Email address: phyweets@nus.edu.sg

[1] M. Yoon, X. F. Lin, I. Chizhov, H. Mai, and R. F. Willis, Phys. Rev. B **64**, 085321 (2001).

[2] J.-L. Li, J.-F. Jia, X.-J. Liang, X. Liu, J.-Z. Wang, Q.-K. Xue, Z.-Q. Li, J. S. Tse, Z. Zhang, and S. B. Zhang, Phys. Rev. Lett. **88**, 066101 (2002).

[3] M. Y. Lai and Y. L. Wang, Phys. Rev. B **64**, 241404(R) (2001).

[4] L. Vitali, M. G. Ramsey, and F. P. Netzer, Phys. Rev. Lett. **83**, 316 (1999).

[5] V. G. Kotlyar, A. V. Zotov, A. A. Saranin, T. V. Kasyanova, M. A. Cherevik, I. V. Pisarenko, and V. G. Lifshits, Phys. Rev. B **66**, 165401 (2002).

[6] J. Jia, J.-Z. Wang, X. Liu, Q.-K. Xue, Z.-Q. Li, Y. Kawazoe, and

S. B. Zhang, Appl. Phys. Lett. **80**, 3186 (2002).
[7] J. M. Gomez-Rodriguez, J. J. Sáenz, A. M. Baró, J.-Y. Veuillen, and R. C. Cinti, Phys. Rev. Lett. **76**, 799 (1996).
[8] I. Chizhov, G. Lee, and R. F. Willis, Phys. Rev. B **56**, 12316 (1997).
[9] J. Myslivecek, P. Sobotik, I. Ost'adal, T. Jarolimek, and P. Smilauer, Phys. Rev. B **63**, 045403 (2001).
[10] Y. P. Zhang, L. Yang, Y. H. Lai, G. Q. Xu, and X. S. Wang, Surf. Sci. **531**, L378 (2003).
[11] P. A. Bennett, M. Copel, D. Cahill, J. Falta, and R. M. Tromp, Phys. Rev. Lett. **69**, 1224 (1992).
[12] J. Alvarez, A. L. Vasquez de Parga, J. J. Hinarejos, J. de la Figuera, E. G. Michel, C. Ocal, and R. Miranda, Phys. Rev. B **47**, 16048 (1993).
[13] M. A. K. Zilani, Y. Y. Sun, H. Xu, L. Liu, Y. P. Feng, X.-S. Wang, and A. T. S. Wee, Phys. Rev. B **72**, 193402 (2005).
[14] R. J. Hamers, R. M. Tromp, and J. E. Demuth, Phys. Rev. Lett. **56**, 1972 (1986).
[15] St. Tosch and H. Neddermeyer, Phys. Rev. Lett. **61**, 349 (1988).
[16] A. L. Ankudinov, B. Ravel, J. J. Rehr, and S. D. Conradson, Phys. Rev. B **58**, 7565 (1998).
[17] H. Xu, Y. G. Li, A. T. S. Wee, C. H. A. Huan, and E. S. Tok, Surf. Sci. **513**, 249 (2002).
[18] X. F. Lin, I. Chizhov, H. A. Mai, and R. F. Willis, Surf. Sci. **366**, 51 (1996).
[19] Y. L. Wang, H. -J. Gao, H. M. Guo, H. W. Liu, I. G. Batyrev, W. E. McMahon, and S. B. Zhang, Phys. Rev. B **70**, 073312 (2004).
[20] P. Sutter, P. Zahl, E. Sutter, and J. E. Bernard, Phys. Rev. Lett. **90**, 166101 (2003).
[21] R. M. Feenstra, J. A. Stroscio, and A. P. Fein, Surf. Sci. **181**, 295 (1987).
[22] R. M. Feenstra, Phys. Rev. B **50**, 4561 (1994).
[23] M. Prietsch, A. Samsavar, and R. Ludeke, Phys. Rev. B **43**, 11850 (1991).
[24] V. G. Kotlyar, A. V. Zotov, A. A. Saranin, E. N. Chukurov, T. V. Kasyanova, M. A. Cherevik, I. V. Pisarenko, H. Okado, M. Katayama, K. Oura, and V. G. Lifshits, Phys. Rev. Lett. **91**, 026104 (2003).
[25] J. G. Norman, Mol. Phys. **31**, 1191 (1976).
[26] H. A. Durr, S. S. Dhesi, E. Dudzik, D. Knabben, G. van der Laan, J. B. Goedkoop, and F. U. Hillebrecht, Phys. Rev. B **59**, R701 (1999).